Open Access

Advances in Environmental and Engineering Research

LIDSEN Publishing Inc.

Original Research

On the Relation between Overwater Friction Velocity and the Wind Speed During Tropical Cyclones

Shih-Ang Hsu *

Coastal Studies Institute, Louisiana State University, USA; E-Mail: sahsu@lsu.edu

* **Correspondence:** Shih-Ang Hsu; E-Mail: sahsu@lsu.edu

Academic Editor: Tomeu Rigo Ribas

Adv Environ Eng Res
2025, volume 6, issue 1
doi:10.21926/aeer.2501007

Received: October 17, 2024
Accepted: January 09, 2025
Published: January 15, 2025

Abstract

In the realm of marine meteorology, physical oceanography, and coastal and ocean engineering, the wind-stress across the air-sea interface plays a dominant role. However, under tropical cyclone conditions, there is no consensus for the formulation of the drag coefficient, C_d, in the literature. Based on the wind-gust method and the measurements from data buoy 42001 during Hurricane Lili, it is demonstrated that, $U_* = 0.073U_{10} - 0.44$, which is valid up to wind speed 47 m s^{-1} and wind gust to 66 m s^{-1}, here U_* is the friction velocity and U_{10} is the wind speed at 10-m height. This formula is also supported by the atmospheric vorticity method. Applications for this proposed formula to estimate the variation of the wind speed with height and to determine the wind-stress storm surge or saltwater flooding during the most recent Hurricane Helene in 2024 are successful. In addition, it is found that $C_d = (1.29Ln(H_s) + 0.27)/1000$, which may be used to explain the behavior of the variation of C_d with the significant wave height, H_s. In order to further substantiate the proposed formula, more datasets during other tropical cyclones are incorporated for the validation.

Keywords

Wind stress at sea; overwater friction velocity; significant wave height; air-sea drag coefficient; hurricane-induced saltwater flooding

1. Introduction

The wind stress or momentum exchange across the air-sea interface is a vital parameter for marine meteorology and physical oceanography (met-ocean). An extensive review on the subject can be found in Bryant and Akbar (2016) [1]. The wind stress, τ, is defined as

$$\tau = \rho_{air} U*^2 = \rho_{air} C_d U_{10}{}^2 \quad (1)$$

Here ρ_{air} (≈1.2 kg m^{-3}) is the air density, $U*$ is the friction velocity, C_d is the drag coefficient, and U_{10} is the wind speed at 10-m height. The units are in SI, unless specified otherwise.

Based on direct measurements, according to Edson et al. ([2], p.1603), for fully rough seas, when U_{10} > 8.5 m s^{-1}, $U*$ > 0.035U_{10} or $U*$ > 0.30 m s^{-1}, and for U_{10} < 25 m s^{-1},

$$U* = aU_{10} + b = 0.062U_{10} - 0.28 \quad (2)$$

Here "a" and "b" are coefficients which need to be determined from field measurements. Edson et al. further stated that although Eq. (2) is not expected to hold for wind speeds associated with tropical cyclones (TCs), it provides additional evidence that the increase of the drag coefficient with winds is already slowing between 20 and 25 m s^{-1}.

Because extreme variations in the wind-stress formulation existed in the literature for strong winds, according to Bryant and Akbar, and U_{10} < 25 m s^{-1} were employed in Edson et al., it is the purpose of this study to alleviate these deficiencies by using wind gust method [3] as measured directly by the National Data Buoy Center (NDBC, available online at www.ndbc.noaa.gov) at the data buoy 42001 during Hurricane Lili with U_{10} over 47 m s^{-1} and gust up to 66 m s^{-1}. This is to see whether Eq. (2) can be extended into hurricane conditions. In addition, resolving the wind-stress formulation for U_{10} > 25 m s^{-1} is needed in met-ocean science and coastal and ocean engineering such as better storm surge forecasting for the evacuation of coastal residents and hindcasting for the assessment of property damages during TCs. In this regard, in 2024, we had Hurricanes Francine and Helene impacted several met-ocean stations in the Gulf of Mexico. Pertinent datasets during these storms and others are also incorporated in this study.

2. Met-Ocean Characteristics of Hurricane Lili

According to the National Hurricane Center (NHC. see www.nhc.noaa.gov/data/tcr/AL132002_Lili.pdf) and the NDBC (www.ndbc.noaa.gov), Hurricane Lili in 2002 impacted Buoy 42001 greatly (see Figure 1) [4]. Table 1 depicts that Buoy 42001 was in the collision course with Lili, indicating its eye passed almost directly. The met-ocean parameters as measured show that U_{10} reached up to 47 and gust to 66 m s^{-1}. According to Hsu ([5], Figure 2), when U_{10} > 9 m/s and -10 < (T_{air} - T_{sea}) < 7°C, the atmospheric stability is neutral. Since our measurements were within these limits, the period as listed in Table 1 was neutral, indicating the mechanical turbulence overpowered the thermal effects so that the logarithmic wind-profile law can be applied. In addition, the absolute difference between wind direction and wave direction was within 100 degrees and the wave steepness, H_s/L_p > 0.020 (here L_p (=1.56 T_p^2) is the peak wave length) (see [6]), wind waves prevailed.

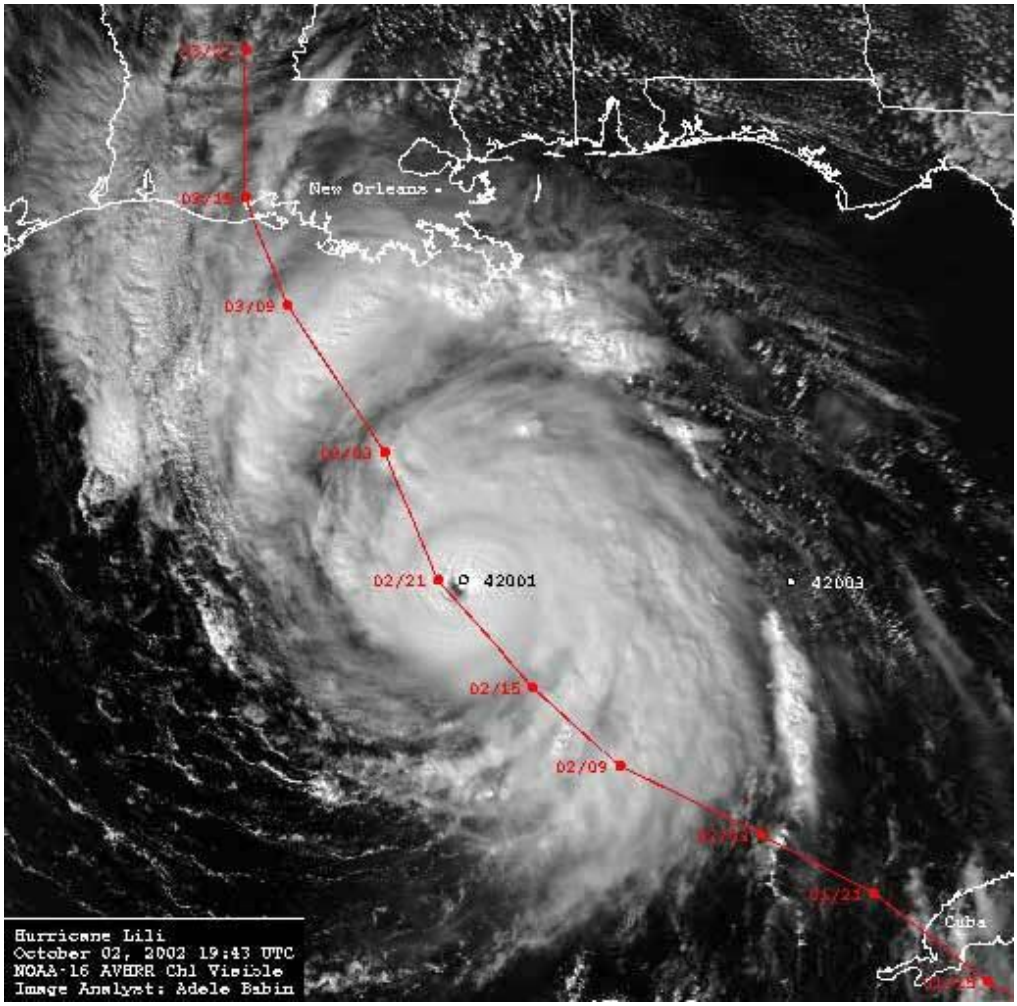

Figure 1 The track of Hurricane Lili in 2002 and the location of Buoy 42001 based on Hsu [6] at https://www.vos.noaa.gov/MWL/spring_03/nowcasting.shtml.

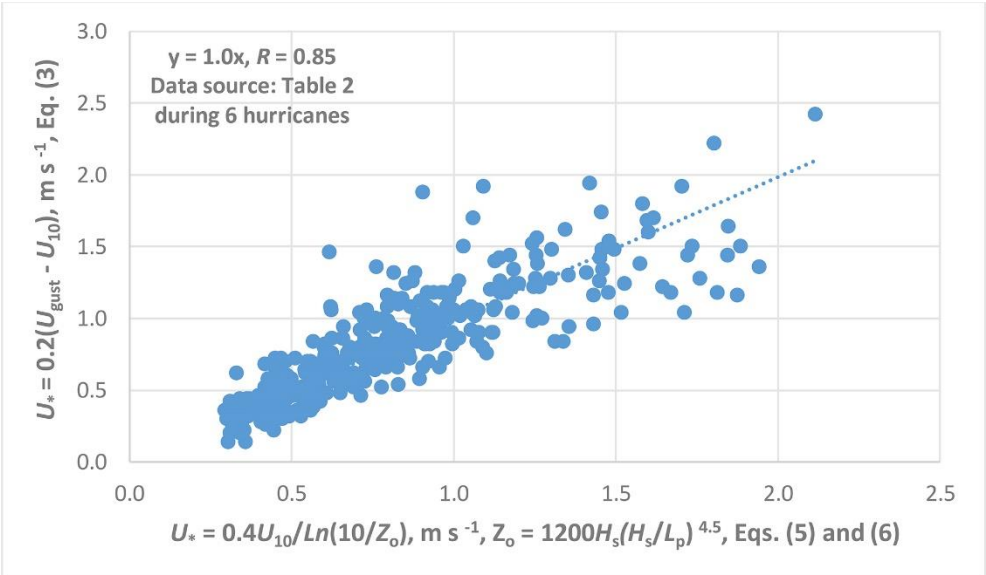

Figure 2 Further verification of Eq. (2) using six hurricanes including Lili.

Table 1 Met-ocean measurements at Buoy 42001 during Hurricane Lili from 2 to 3 Oct 2002 (data source: www.ndbc.noaa.gov). Here U_{gust} is the wind gust, H_s is the significant wave height, T_p is the peak wave period, Baro stands for the barometric pressure in millibar or hPa, and T_{air}, T_{sea} and T_{dew} are for air, sea and dew-point temperatures, respectively.

Hour, UTC	wind Dir.	U_{10}, m/s	U_{gust}, m/s	H_s, m	T_p, sec	wave dir.	Baro mb	T_{air}, degC	T_{sea}, degC	T_{dew}, degC
0	75	9.5	10.7	1.34	5.88	69	1012.5	28	28.2	24.2
1	74	11.7	13.2	1.5	6.25	69	1012.3	27.9	28.2	23.9
2	64	11.9	13.7	1.58	5	75	1012.7	28	28.2	24
3	62	10.9	13.8	1.72	5.88	66	1012.8	27.9	28.2	24.2
4	58	12.1	14.5	1.91	5.88	73	1012.7	28	28.1	24
5	54	11.8	14.5	2	6.67	80	1012.1	27.2	28.1	24.1
6	57	11.5	13.2	2.13	7.69	90	1011.2	27.4	28.1	23.5
7	64	12.7	14.8	2.17	7.69	97	1010.6	27.8	28.1	23.4
8	53	12.5	14.6	2.41	7.69	96	1009.1	27.8	28	23.9
10	67	13.5	16.1	2.73	7.14	74	1008.1	26.7	28	22.6
11	55	14.9	19.1	3.31	9.09	94	1007.4	28	28	24
12	49	14.8	17.4	3.98	10.81	106	1006.6	27.7	28	24.1
13	58	13.1	15.5	4.26	12.12	106	1006.7	25.9	28	23.1
14	51	14.6	16.9	4.75	12.9	108	1006.5	24.1	28	22
15	44	16.5	20.6	4.88	12.12	110	1004.8	26.1	28	23.1
16	48	16.1	23.4	5.35	12.12	108	1003.3	26.2	28	23.3
17	63	23.3	28.9	6.66	13.79	112	1000.3	25.6	28	22.9
18	61	26.7	32.8	7.65	12.9	106	995.1	25.1	27.9	24.5
19	59	32	39.1	8.88	13.79	111	984.6	25.6	27.9	25.2
Eye	103	47.2	65.6	10.22	13.79	111	956.1	25.9	27.6	25.4
21	158	33.7	40.5	11.2	12.9	110	975.4	25.7	27.1	25.5
22	178	25.1	32.5	7.29	10.81	112	988.4	25.7	26.9	24.5
23	190	20.7	24.5	5.69	9.09	229	994.2	26	27	24.2
0	195	19.5	26.3	4.61	10.81	95	998	27.3	27	24.4
1	200	17	21.5	4.33	7.14	223	1001.1	26.5	26.8	23.9
2	199	16.2	20.3	3.77	6.67	211	1003.6	26.8	26.4	23.9
3	191	16	19.2	3.43	7.69	248	1004.9	26.7	26.3	23.8
4	190	15.4	18	3.18	6.67	212	1006.7	27.1	26	24
5	186	13.8	16.6	3.38	6.67	201	1007.2	27.4	25.9	24.3
6	192	12.1	14.1	3.14	7.14	210	1007.4	27.4	26.2	24.4
7	184	14.2	16.6	3.08	7.14	238	1007.2	26.2	26.3	23.1
8	192	12.3	15.1	2.8	6.67	197	1007.2	26.8	26.2	24.2
9	191	10.5	12	2.67	6.67	213	1007.6	27.5	26.2	24.5

3. Methods

The wind gust method used in this study is based on Hsu (2003b, Equations 16 and 17) [3] and Hsu and Blanchard ([7], Eq.8) that

$$U* = 0.2\left(U_{gust} - U_{10}\right) \tag{3}$$

In boundary-layer meteorology the well-known logarithmic wind-profile law (see, e.g. [3]), under neutral stability conditions, is

$$U_z = (U*/k)Ln(Z/Z_o), or \tag{4}$$

by setting Z = 10 m, we have

$$U* = kU_{10}/Ln(10/Z_o) \tag{5}$$

And, according to Taylor and Yelland [8],

$$Z_o/H_s = 1200(H_s/Lp)^{4.5} \tag{6}$$

Here U_z is the wind speed at height Z, k (=0.4) is the von Karman constant, and Z_o is the roughness length.

In order to compare Equations (3) an (4), following datasets during Hurricane Dorian in 2019 are employed: According to the NHC (AL052019_Dorian_final_20200427 (noaa.gov), p.23), at USAF Tower 313 at 0657 UTC on 4 Sep 2019, the 1-minute wind speed and its gust were: at Z_1 = 16 m, U_1 = 44 kts (22.7 m s^{-1}), U_{1gust} = 62 kts (32.0 m s^{-1}) and at Z_2 = 90 m, U_2 = 60 kts (30.9 m s^{-1}) and U_{2gust} = 70 kts (36.1 m s^{-1}).

By eliminating Z_o from Eq. (4) at two levels for Z_1 and Z_2, one gets

$$U* = k(U_2 - U_1)/Ln(Z_2/Z_1) \tag{7}$$

Now, by substituting appropriate values as measurements at 16 m into Eq. (3), $U*$ = 1.86 m s^{-1} and into Eq. (7), $U*$ = 1.90 m s^{-1}, indicating that the wind-gust method is consistent with logarithmic wind-profile approach. In order to further substantiate Eq. (3), more datasets as listed in Table 2 are analyzed using Equations (5) and (6) against (3) and presented in Figure 2. Since the slope is near unity and the correlation coefficient is 0.85, indicating that our wind-gust method is reasonable to use in this study.

Table 2 Simultaneous measurements of U_{10}, U_{gust}, H_s, and T_p for wind seas during 6 hurricanes based on www.ndbc.noaa.gov.

Hurricane name	Month/Year	From	To	NDBC Buoy
Kate	Nov/1985	0200 UTC on 19	2300 UTC on 21	42003
Lili	Oct/2002	2200 UTC on 01	0900 UTC on 03	42001
Ivan	Sep/2004	0800 UTC on 13	1100 UTC on 16	42003
Katrina	AUG/2005	1500 UTC on 26	0500 UTC on 28	42003
Wilma	OCT/2005	1200 UTC on 19	0200 UTC on 24	42056

Ike	Sep/2008	0050 UTC on 10	1350 UTC on 13	42001

4. Results and Verifications

4.1 Relation between U_* and U_{10}

Figure 3 shows the relation between U_* and U_{10} that

$$U_* = 0.073U_{10} - 0.44, or \tag{8}$$

$$C_d = (U_*/U_{10})^2 = (0.073 - 0.44/U_{10})^2 \tag{9}$$

With a correlation coefficient, R = 0.91, which is valid for U_{10} up to 47 m s^{-1}.

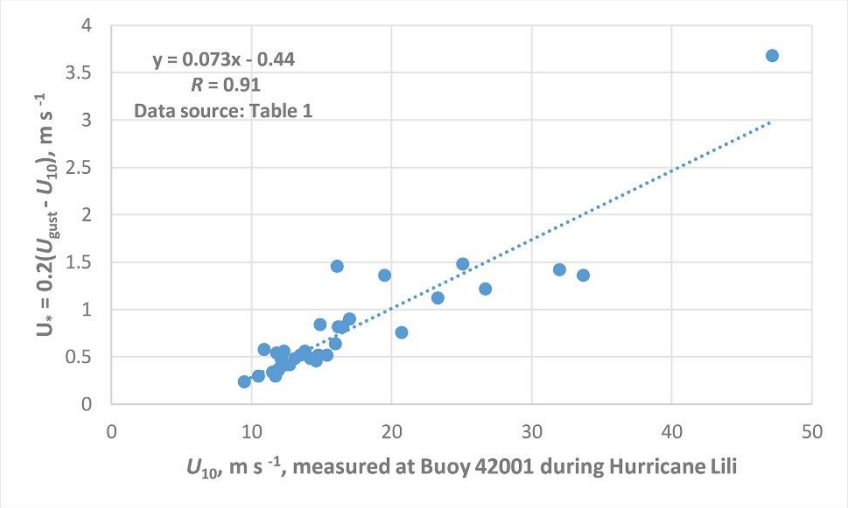

Figure 3 Relation between U_* and U_{10} based on the wind-gust method (Eq. 3).

Verifications of Eq. (8) against other methods are presented from Figures 4 through 7 based on the pertinent datasets provided in the literature from [9-12]. If one accepts the statistics indicated in these figures, Eq. (8) is verified for practical use.

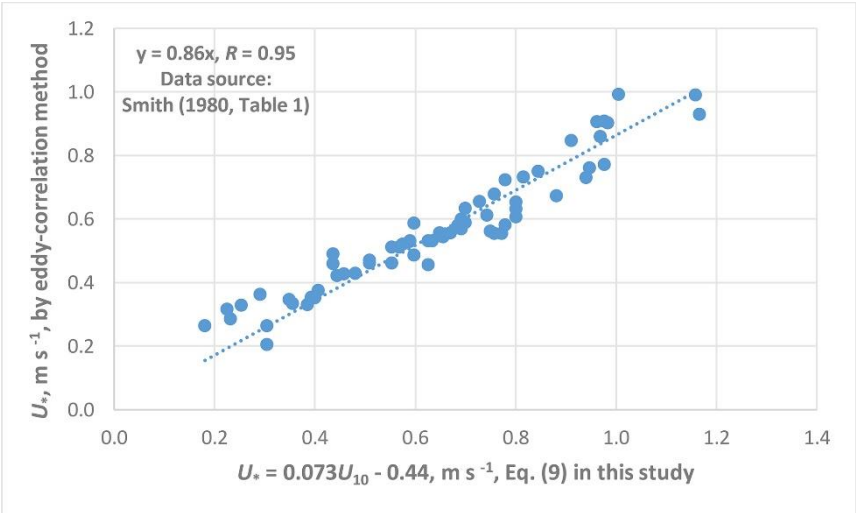

Figure 4 Verification of Eq. (8) against the direct measurements by Smith [9].

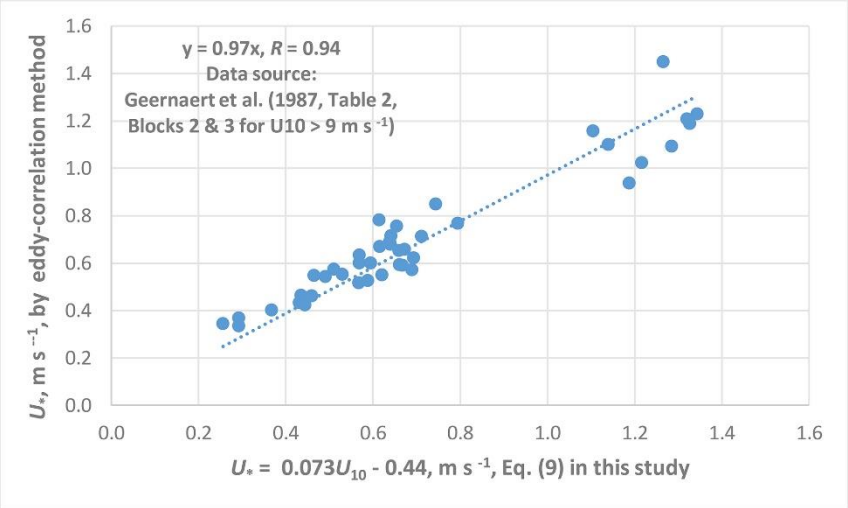

Figure 5 Verification of Eq. (8) against the direct measurements by Geernaert et al. [10].

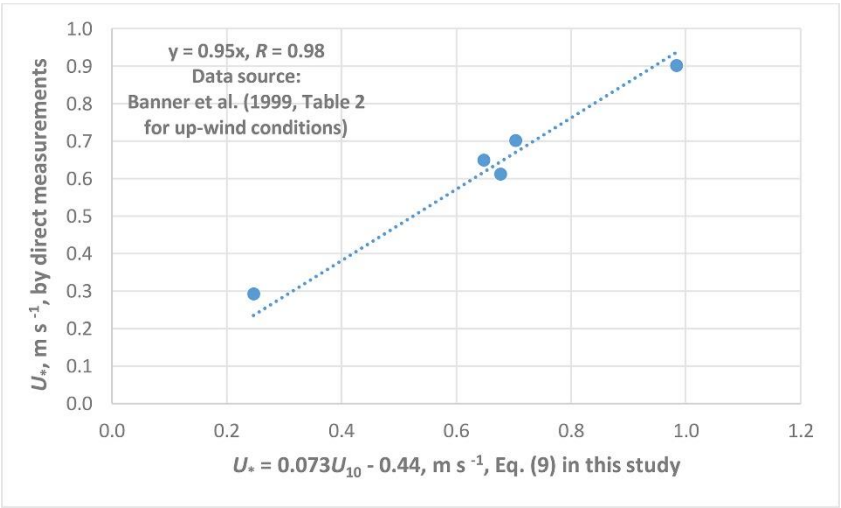

Figure 6 Verification of Eq. (8) against the direct measurements by Banner et al. [11].

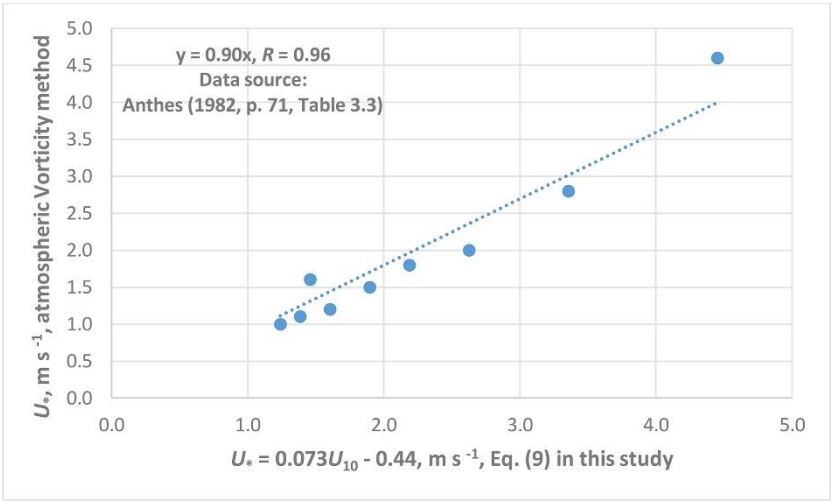

Figure 7 Verification of Eq. (8) against the atmospheric vorticity method by Anthes [12].

A graphic representation of Eq. (9) is presented in Figure 8. Equations (8) and (9) indicate that the generic form of Eq. (2) can now be extended into hurricane conditions and that the increase of the drag coefficient with winds is already slowing between 20 and 25 m s^{-1} as mentioned in the introduction is further confirmed.

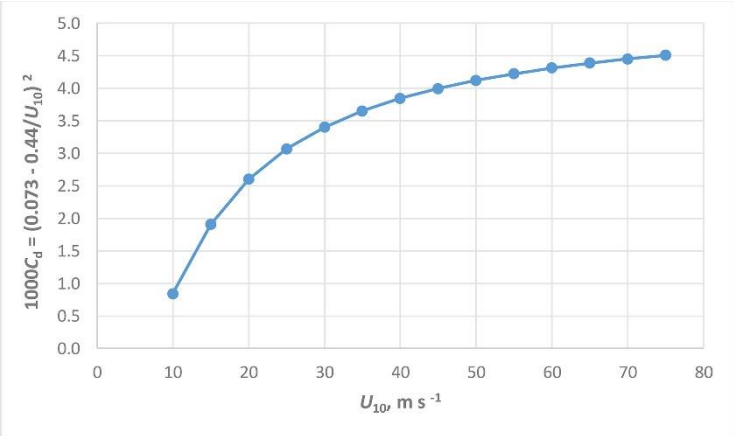

Figure 8 A graphic representation of Eq. (9) (using every 5 m s^{-1} interval for U_{10}).

4.2 Relation between U∗ and H_s

In order to related $U*$ and H_s, Figure 9 is presented that

$$U* = 0.17H_s \tag{10}$$

With R = 0.88.

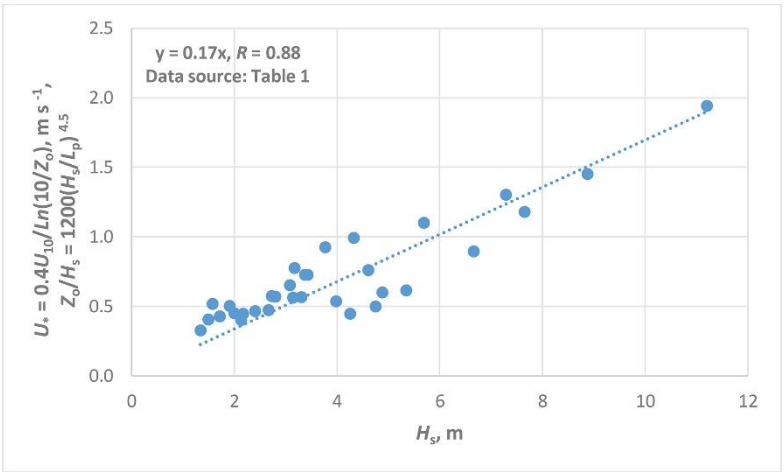

Figure 9 A relation between $U*$ and H_s based on Table 1 (except inside the eye).

4.3 Relation between H_s and U_{10}

From Equations (8) and (10), we have

$$H_s = 0.43U_{10} - 2.6, or \tag{11}$$

$$U_{10} = 2.33H_s + 6 \tag{12}$$

Eq. (12) is further verified as shown in Figure 10.

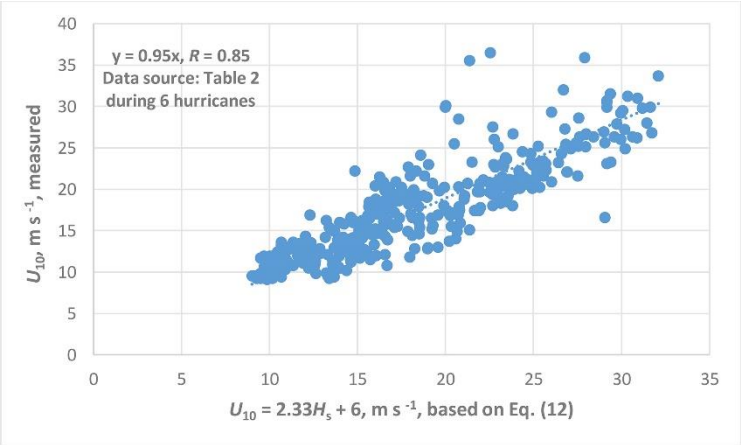

Figure 10 A validation of Eq. (12) using the datasets provided in Table 2.

5. Applications

5.1 Estimatng the Variation of Wind Speed with Height

Rearranging Eq. (7), we have

$$U_2 = U_1 + (U*/k)Ln(Z_2/Z_1) \tag{13}$$

And substituting U_* from Eq. (10) into Eq. (13) and set k = 0.4, one gets

$$U_2 = U_1 + 0.43H_sLn(Z_2/Z_1) \tag{14}$$

A validation of Eq. (14) is presented in Figure 11 at NDBC Buoy 42036 which was impacted by Hurricane Helene in September 2024 (for location, see www.ndbc.noaa.gov). For a rapid estimation of U_{10} from $U_{3.8}$ as measured by this buoy, see Figure 12 that

$$U_{10} = 1.1U_{3.8} \tag{15}$$

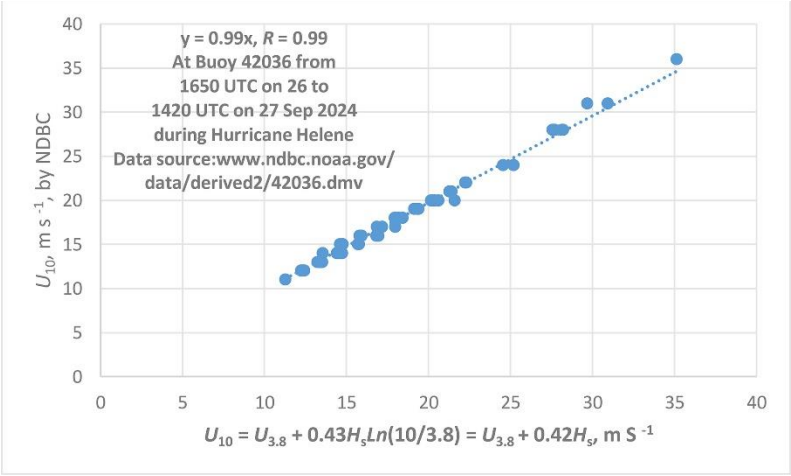

Figure 11 Further verification of Eq. (14).

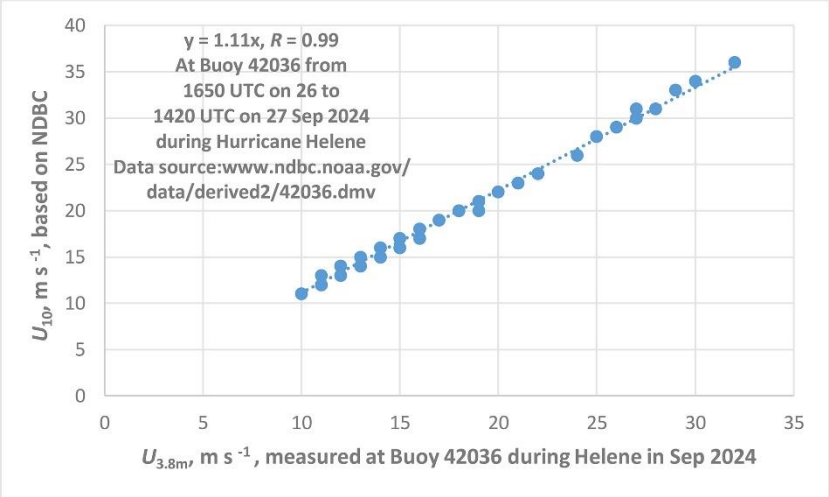

Figure 12 A rapid estimation of U_{10} from $U_{3.8}$.

Since there are instances that only H_s is available but one still needs the estimation of the wind speed at different elevation other than U_{10}, this can be accomplish as follows:

By setting U_2 as U_z and U_1 as U_{10} into Eq. (14) and using Eq. (12), we have

$$U_z = (2.33H_s + 6) + 0.43H_sLn(Z/10) \tag{16}$$

During Hurricane Francine in Sep 2024 (see www.nhc.noaa.gov, The Louisiana Offshore Oil Port (LOPL1) (for location, see www.ndbc.noaa.gov) was impacted. Since the anemometer is located at Z = 57.9 m above the sea surface and using the H_s measurements at this facility, the wind speed can be estimated and verified in Figure 13.

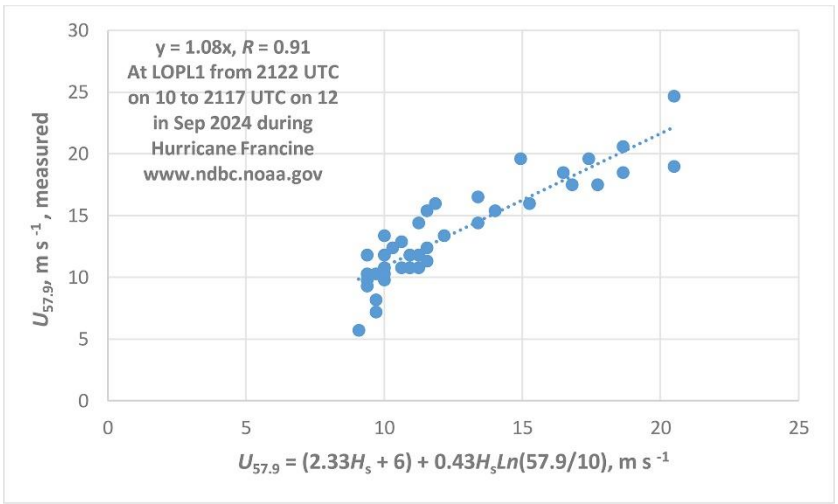

Figure 13 A verification of Eq. (20) at LOPL1 impacted by Hurricane Francine in 2024.

5.2 Estimating the Wind-Stress Induced Storm Surge

The storm surge induced by the wind stress, also called saltwater flooding in layman's term, is simplified (see, e.g., [13]), based on Eq. (1), that

$$\rho_{sea}gD\ dS/dX = \tau = \rho_{air}U*^2 = \rho_{air}C_d{U_{10}}^2 = 1.2(0.2(U_{gust} - U_{10})^2) \tag{17}$$

Here ρ_{sea} is the density of seawater, g is the gavitational acceleration, D is the water depth, dS/dX is the water slope in which S is the water level along the onshore distance X. Eq. (17) indicates that the seawater slope or storm surge (a surrogate for the potential energy) is balanced by the wind stress (a surrogate for the kinetic energy).

In September 2024, Hurricane Helene devasted the "Big Bend" area, Florida with over 3 m (10 ft) saltater flooding. According to RAMMB, the track of Helene is shown in Figure 14 and isotach analysis in Figure 15, respectively. Figure 16 illustrates the forecast peak storm surge in ft (note: 1 m = 3.281 ft) by the NHC.

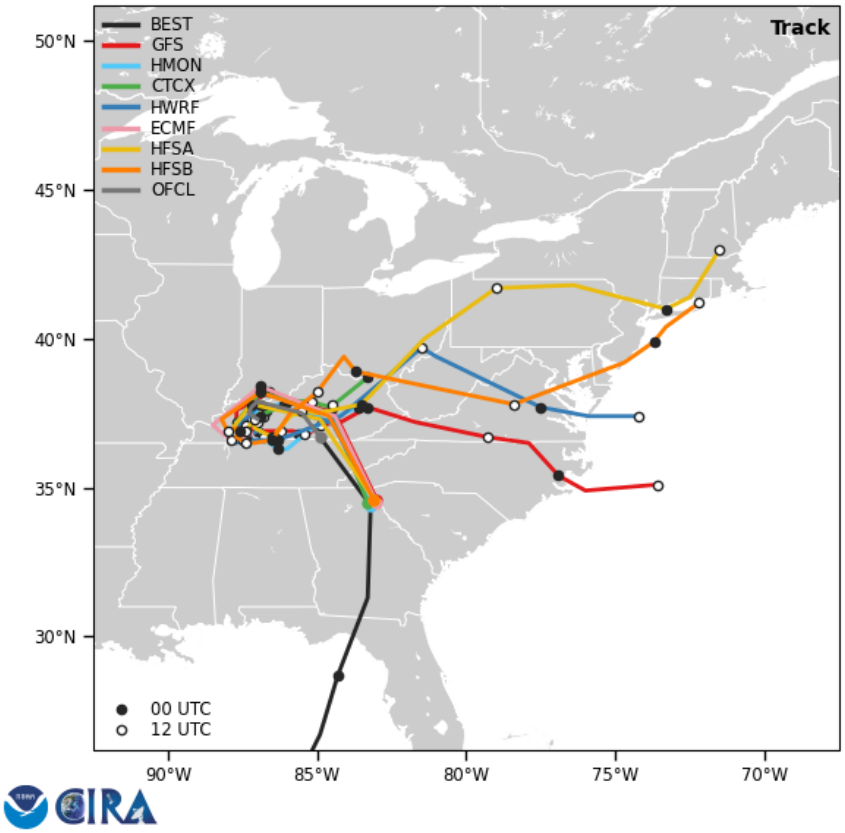

Figure 14 A portion of storm track over the Gulf of Mexico during Hurricane Helene in September 2024, based on https://rammb-data.cira.colostate.edu/tc_realtime/products/storms/2024al09/diagplot/2024al09_diagplot_202409271800.png.

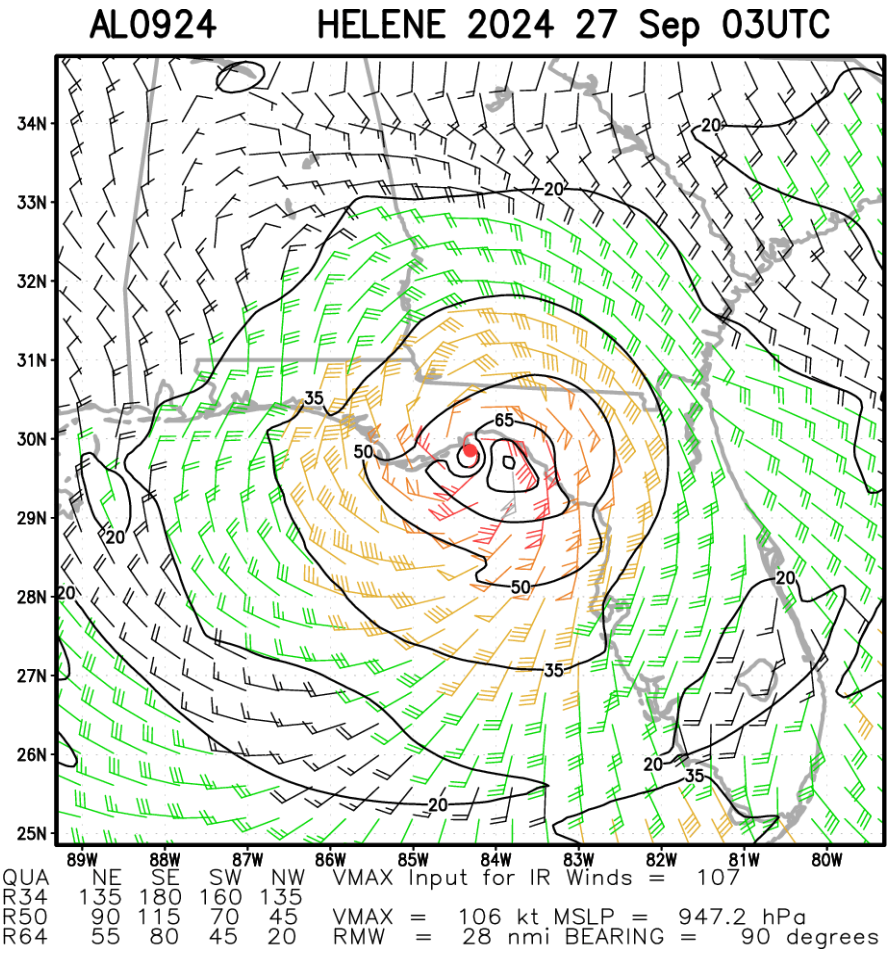

Figure 15 The spatial distribution of the isotach (lines of equal wind speed in knots (note: 1 m s^{-1} = 1.94 knot)) near the landfall of Helene on the "big Bend" area in Florida based on https://rammb-data.cira.colostate.edu/tc_realtime/products/storms/2024al09/mpsatwnd/2024al09_mpsatwnd_202409270300_swnd.gif.

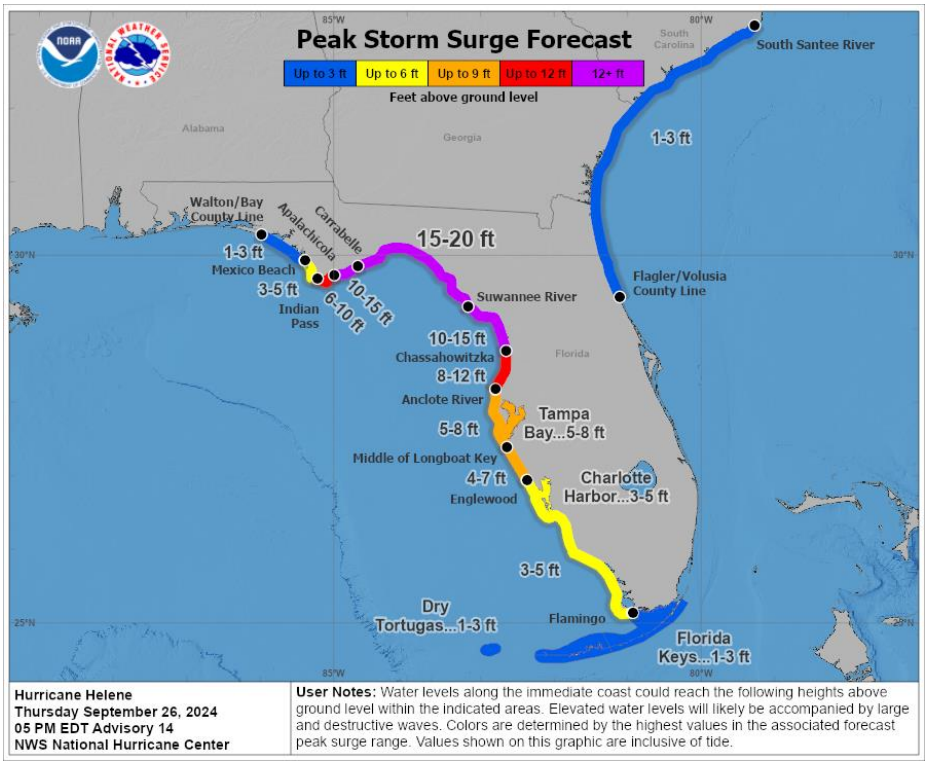

Figure 16 Peak storm surge forecast for Hurricane Helene in September 2024 based on https://www.nhc.noaa.gov/storm_graphics/AT09/refresh/AL092024_peak_surge+png/211601_peak_surge.png.

Note that the isotach analysis similar to Figure 14 has been available since 2006 as issued by RAMMB for tropical cyclones worldwide, it is employed here for rapid estimation of saltwater flooding. In order to facilitate these estimation, Table 3 is presented. It can be seen that using this table along with Figure 15, our rapid estimation method is consistent with the peak storm surge forecast as depicted Figure 16 which is based on extensive computer modeling. Note also that the software used in Figure 15 and Figure 16 are from RAMMB and NHC, they cannot be juxtaposed with each other at this time.

Table 3 Rapid estimation of seawater flooding based on the isotach analysis by RAMMB.

Isotach, kt	Isotach, m s^{-1}	C_d, Eq. (11)	Seawater flood, m	Seawater flood, ft
35	18.0	0.0024	0.93	3
50	25.8	0.0031	2.48	8
65	33.5	0.0036	4.85	16
80	41.2	0.0039	7.94	26

In order to further demonstrate the usefulness of Eq. (17) for saltwater flooding estimates, the wind measurements during Helene at Cedar Key, Florida (CKYF1, located just south of Suwannee River as shown in Figure 16, and for its exact location see www.ndbc.noaa.gov), are employed. Figure 17 shows the measurements of wind speed and its associated gust at 10.3 m.

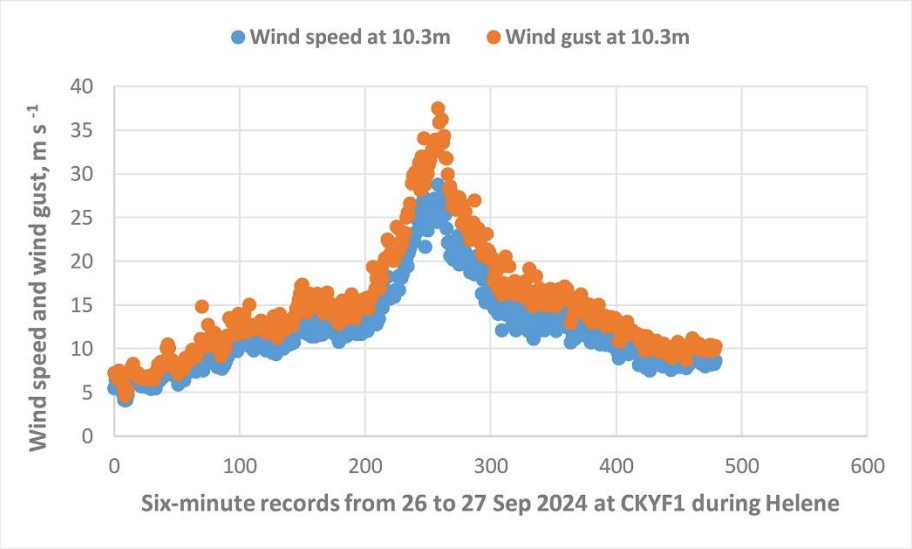

Figure 17 Measurements of wind speed and its gust at 10.3 m at CKYF1 during Helene.

Using the computed values of U_* as provided in Figure 18, characteristics of the storm surge at CKYF1 is demonstrated in Figure 19. Since the estimated seawater flooding is approximately 10 ft and by adding the 3 ft astronomical tide, the total peak water level is 13 ft, which is consistent to the forecast peak storm surge of 10 to 15 range by the NHC as indicated in Figure 16 in area just south of Suwannee River where the met-ocean station CKYF1 is located.

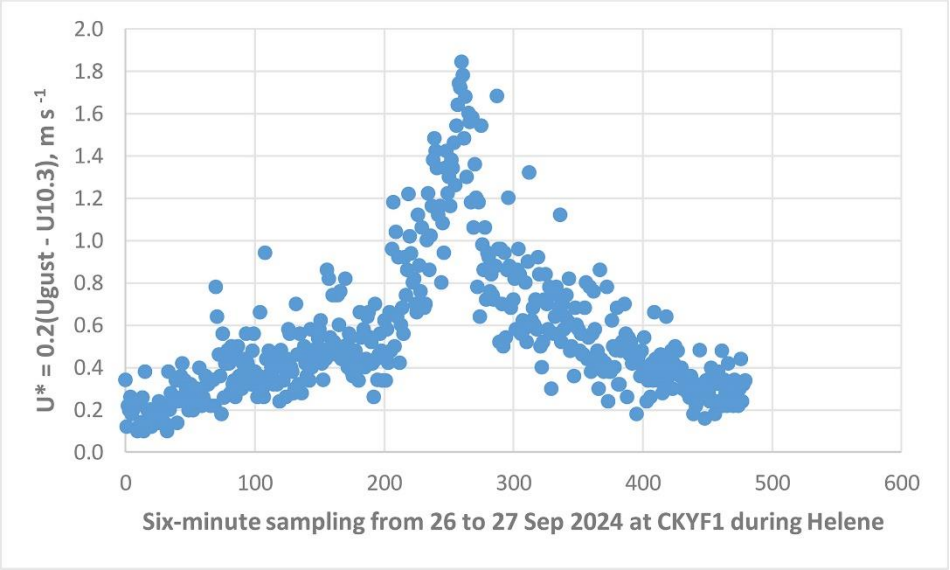

Figure 18 Estimates of U_* at CKYF1 during Helene.

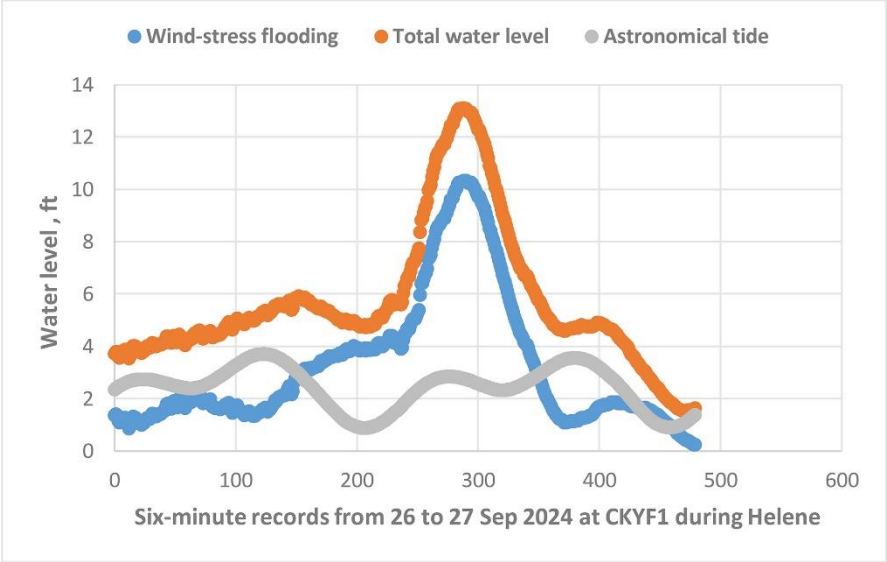

Figure 19 Temporal variations of seawater flooding, astronomical tides and total water level at CKYF1 during Helene.

5.3 Relation between C_d and H_s

Finally, based on aforementioned analysis and discussion, we are now able to resolve the longtime dispute among scientists and engineers on the variation of C_d with U_{10} during a tropical cyclone as set forth in the introduction:

By substituting Eq. (12) into Eq. (9), we have

$$C_d = (0.073 - 0.44/(2.33H_s + 6))^2/1000 \tag{18}$$

Eq. (18) can be further simplified as depicted in Figure 20 that

$$C_d = (1.29Ln(H_s) + 0.27)/1000 \tag{19}$$

With coefficient of determination R^2 = 0.99 or R = 0.99.

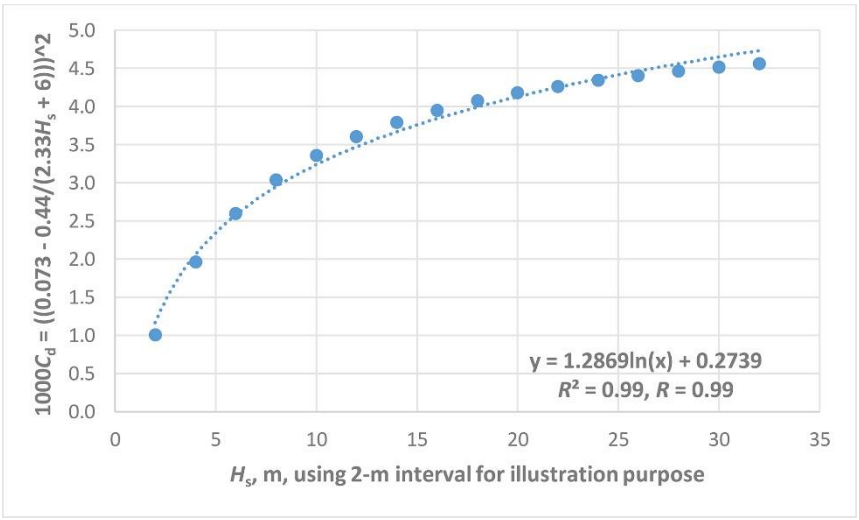

Figure 20 A relation between C_d and H_s.

According to Holthuijsen et al. (2012) [14], the saturation of wave streaks occurred around U_{10} = 40 m s^{-1} or approximately H_s = 15 m based on Eq. (11). Therefore, for H_s > 15 m, the wind is not only drag the actual waves but also the sea forms and wave streaks so that the slope slows down more as depicted in Figure 20.

An application of Eq. (19) is presented as follows: According to Bancroft [15], during Super-Typhoon Soudelor in 2015, an extreme value of H_s = 27.6 m was measured. By substituting this value into Eq. (19), we have C_d = 0.0045, and Eq. (10), U_* = 4.7 m s^{-1}. Therefore, $U_{10} = U_*/C_d^{0.5}$ = 70 m s^{-1}, which is in excellent agreement with the measured near surface wind speed of 72 m s^{-1} as stated in [15].

6. Conclusions

On the basis of aforementioned analysis and discussion, it is concluded that the wind-stress induced drag coefficient can be formulated up to the 47 m s^{-1} uing the wind gust method (see Equations 8 and 9 based on six hurricanes as listed in Table 2). The magnitute of wind-stress induced storm surge or saltwater flooding can be estimated by Eq. (17), which is also verified by the most recent Hurricane Helene in 2024 by both the extensive computer modeling by the NHC as well as at a coastal met-ocean station impacted by the storm. Using the wind-wave-friction velocity relations as presented in this study, our proposed wind-stress drag coefficient formulation can also be linked to the wave effects including the actural wind waves, wave streaks and sea forms as depicted in Eq. (19) and Figure 20 for the slow-down behavior of the drag coefficient. An application of Eq. (19) during an extreme wave condition induced by a super typhoon is also presented.

Acknowledgments

Appreciation goes to the NDBC, NHC, NOS and RAMMB for providing the datasets and pertinent graphs and charts used in this research.

Author Contributions

The author did all the research work of this study.

Competing Interests

The author has declared that no competing interests exist.

References

1. Bryant KM, Akbar M. An exploration of wind stress calculation techniques in hurricane storm surge modeling. J Mar Sci Eng. 2016; 4: 58.
2. Edson JB, Jampana V, Weller RA, Bigorre SP, Plueddemann AJ, Fairall CW, et al. On the exchange of momentum over the open ocean. J Phys Oceanogr. 2013; 4: 1589-1610.
3. Hsu SA. Estimating overwater friction velocity and exponent of power-law wind profile from gust factor during storms. J Waterw Port Coast Ocean Eng. 2003; 129: 174-177.

4. Hsu SA. Nowcasting the wind speed during a hurricane at sea [Internet]. College Park, MD: National Center for Environmental Prediction; 2003. Available from: https://www.vos.noaa.gov/MWL/spring_03/nowcasting.shtml.
5. Hsu SA. An overwater stability criterion for the offshore and coastal dispersion model. Boundary Layer Meteorol. 1992; 60: 397-402.
6. Hsu SA, He Y, Shen H. Buoy measurements of wind--wave relations during hurricane Matthew in 2016. J Phys Oceanogr. 2017; 47: 2603-2609.
7. Hsu SA, Blanchard BW. Estimating overwater turbulence intensity from routine gust-factor measurements. J Appl Meteorol Climatol. 2004; 43: 1911-1916.
8. Taylor PK, Yelland MJ. The dependence of sea surface roughness on the height and steepness of the waves. J Phys Oceanogr. 2001; 31: 572-590.
9. Smith SD. Wind stress and heat flux over the ocean in gale force winds. J Phys Oceanogr. 1980; 10: 709-726.
10. Geernaert GL, Larsen SE, Hansen F. Measurements of the wind stress, heat flux, and turbulence intensity during storm conditions over the North Sea. J Geophys Res Oceans. 1987; 92: 13127-13139.
11. Banner ML, Chen W, Walsh EJ, Jensen JB, Lee S, Fandry C. The Southern Ocean waves experiment. Part I: Overview and mean results. J Phys Oceanogr. 1999; 29: 2130-2145.
12. Anthes RA. Tropical cyclones, their evolution, structure and effects. Meteorological monographs. Ephrata, PA: American Meteorological Society, Science Press; 1982.
13. Hsu SA, Grymes JM, Yan Z. A simplified hydrodynamic formula for estimating the wind-driven flooding in the lake Pontchartrain-Amite river basin. Natl Weather Dig. 1997; 21: 18-22.
14. Holthuijsen LH, Powell MD, Pietrzak JD. Wind and waves in extreme hurricanes. J Geophys Res Oceans. 2012; 117. doi: 10.1029/2012JC007983.
15. Bancroft GP. Marine weather review - North Pacific Area March to August 2015 [Internet]. College Park, MD: National Center for Environmental Prediction; 2016. Available from: https://www.vos.noaa.gov/MWL/201604/northpacific.shtml#contents.